Physical Drivers of Thin Snowpack Spatial Structure from Unpiloted Aerial System (UAS) Lidar Observations

Eunsang Cho[1,2*†], Adam G. Hunsaker[1,2], Jennifer M. Jacobs[1,2], Michael Palace[2,3], Franklin B. Sullivan[2], Elizabeth A. Burakowski[2]

[1]Department of Civil and Environmental Engineering, University of New Hampshire, Durham, NH, USA
[2]Earth Systems Research Center, Institute for the Study of Earth, Oceans, and Space, University of New Hampshire, Durham, NH, USA
[3]Department of Earth Sciences, University of New Hampshire, Durham, NH, USA

[†]Eunsang Cho's current affiliations are Hydrological Sciences Laboratory, NASA Goddard Space Flight Center, Greenbelt, MD, USA, and Earth System Science Interdisciplinary Center, University of Maryland, College Park, MD, USA

[*]Corresponding author: Eunsang Cho (ec1072@wildcats.unh.edu)

Highlights

- Dominant physical drivers of the snowpack spatial patterns from UAS-based lidar were identified using the Maximum Entropy (MaxEnt) framework
- Plant functional type and terrain roughness contribute up to 80% and 76% of the relative importance in MaxEnt across the landscape
- Soil variables were also important controls suggesting soils can control thermal transfer among soil, snowpack, and surface-atmosphere

Submitted to *Water Resources Research*

December 15, 2020

Abstract

Snow distribution is a function of interactions among static variables, such as terrain, vegetation, and soil properties, and dynamic meteorological variables, such as wind speed and direction, solar radiation, and soil moisture that occur over a range of spatial scales. However, identifying the dominant physical drivers responsible for spatial patterns of the snowpack, particularly for ephemeral, shallow snowpacks, has been challenged due to the lack of the high-resolution snowpack and physical variables with high vertical accuracy as well as inherent limitations in traditional approaches. This study uses an Unpiloted Aerial System (UAS) lidar-based snow depth and static variables (1-m spatial resolution) to analyze field-scale spatial structures of snow depth and apply the Maximum Entropy (MaxEnt) framework to identify primary controls over open terrain and forests at the Thompson Farm Research Observatory, New Hampshire, United States. We found that, among nine topographic and soil variables, plant functional type and terrain roughness contribute up to 80% and 76% of relative importance in MaxEnt to predicting locations of deeper or shallower snowpacks, respectively, across the landscape. Soil variables, such as organic matter and saturated hydraulic conductivity, were also important controls (up to 70% and 81%) on snow depth spatial variations for both open and forested landscapes suggesting spatial variations in soil variables under snow can control thermal transfer among soil, snowpack, and surface-atmosphere. This work contributes to improving land surface and snow models by informing parameterization of the sub-grid scale snow depths, down-scaling remotely sensed snow products, and understanding field scale snow states.

1. Introduction

Snow plays a significant role in hydrologic and ecological processes globally (Barnett et al., 2005). It also benefits much of the world’s population from climate services through the retention of water for release during seasonally dry periods and land surface energy budgets (Sturm et al., 2017). Snowpack structure and evolution determine snowmelt runoff, infiltration, and groundwater recharge (Carroll et al., 2019; Earman et al., 2006; Harpold et al., 2015; Lundquist et al., 2004; Maurer and Bowling, 2014). Snow plays an important role in partitioning incoming solar radiation and longwave radiation into outgoing longwave radiation, and latent heat, ground heat, and sensible heat fluxes (Ge and Gong, 2010; Lawrence and Slater, 2010;

Liston, 1999; Stieglitz et al., 2001). Snow's insulating properties control the underlying soils' freeze-thaw state (Groffman et al., 2001; Starkloff et al. 2017; Yi et al. 2019) affecting soil respiration, carbon sequestration, nutrient retention, and microbial communities (Aase and Siddoway, 1979; Isard and Schaetzel, 1998; Monson et al., 2006; Henry, 2008; Aanderud et al., 2013; Tucker et al., 2016; Sorensen et al., 2018; Reinmann and Templer, 2018). In addition to the total amount of snow, the spatial nonuniformity of snow exerts a strong control on processes for patchy snow in shallow ephemeral snowpacks (Anderton et al., 2002; Lundquist and Dettinger, 2004; Schlogl et al. 2018). When interactions among terrain, vegetation, and soils and snowpack are captured, they can also be useful in parameterizing the sub-grid scale in snow models to improve model accuracy (Luce et al., 1999; Sturm and Wagner, 2010) or to downscale remotely sensed snow products (e.g., radar backscatter, passive microwave, and gamma radiation; Cho et al., 2020; Derksen et al., 2010; Lemmetyinen et al., 2016; Saberi et al., 2020) that are too coarse to provide an understanding of conditions at field scales.

The spatial variability in snow depth is a function of static and dynamic conditions over a range of spatial scales (Clark et al., 2011). Fixed physical controls including terrain (Blöschl and Kirnbauer, 1992; Lapen and Martz, 1996; Mott et al., 2011), vegetation (Gelfan et al., 2004; DeBeer and Pomeroy, 2010; Currier and Lundquist, 2018), and even soil (Mott et al., 2013; Shook et al., 1993; Pomeroy et al., 1998) are primary controls for variations in snow depth and snow water equivalent at multiple scales across the landscape. In the absence of major vegetation interactions, terrain elevation, slope, aspect, and roughness can control accumulation and ablation patterns, with greater accumulation at higher elevations (Grünewald and Lehning, 2011), reduced snow depth on steep slopes (Blöschl and Kirnbauer, 1992), lee slope loading with preferential wind deposition of precipitation (Mott et al. 2011), retention of snowpack on north facing slopes during the ablation season (Gray and Male, 1981; Schirmer and Pomeroy, 2020), and rougher terrain holding less snow than smoother terrain (Lehning et al., 2011). With tall vegetation, canopy interception by coniferous forests (30-79%) can reduce accumulation on the ground (McNay et al. 1988; Schmidt and Gluns, 1991; Pomeroy and Gray, 1995; Storck et al. 2002; Roth and Nolin, 2017, and others), though the magnitude of canopy interception depends on storm type and canopy crown completeness. Less is known about deciduous forest canopy interception, which ranges from 1% based on a hardwood forest study in Japan (Nakai et al. 1993) and up to 25% in a southern beech forest in Peru (Huerta et al. 2019). Vegetation can also affect snow spatial variability during the ablation season through canopy shading (Essery et al. 2008; Musselman et al. 2008) and reduced sublimation (Roth and Nolin, 2017). Many western U.S. studies have identified elevation and temperature as primary factors explaining differences in forested versus open snowpack accumulation and duration (Lundquist et al., 2013; Roth and Nolin, 2017). For soil-snow interactions, previous work indicates that the spatial distribution of snowpack and melt timing controlled spatial patterns in soil moisture and temperature (Shook et al., 1993; Mott et al., 2013). However, there is limited research regarding if and how soil property spatial variations contribute to snow distribution during the accumulation and ablation periods.

Traditional manual ground sampling methods have been used to characterize snow depth spatial variability using statistical indicators, probability distributions, and fractal methods. Using traditional point measurements with limited sample size requires a balance between the sampling spatial extent and sample density. This impacts the ability to capture spatial variability that naturally increases with spatial scale as compared to capturing small-scale spatial structures (Clark et al. 2011). Remote sensing methods provide the ability to collect data over a continuous spatial extent, thus expanding on the understanding of snow distribution (Broxton et al., 2019; Deems et al., 2006; Painter et al., 2016; Jacobs et al., 2020; Tinkham et al., 2014).

Over the past two decades, airborne remote sensing methods, providing spatially continuous, high-resolution snow depth maps at local and regional scales, have greatly advanced the ability to characterize the spatiotemporal variability of snow depth over earlier work using snow probes (see reviews in Deems et al., 2013; López-Moreno et al., 2017). Airborne laser scanning (ALS) (Deems et al., 2013; Harpold et al., 2014; Kirchner et al., 2014), terrestrial laser scanning (TLS) (Grünewald et al. 2010; Currier et al. 2019), and structure-from-motion photogrammetry (SfM) (Nolan et al., 2015; Bühler et al., 2016; Goetz and Brenning, 2019) have emerged as viable methods to map surface elevations with snow-off and snow-on conditions in order to differentially map snow depths.

Many snowpack patterns are controlled by fixed physical controls including vegetation and topography that are relatively consistent from year to year (i.e., time stable; Grayson et al. 2002; Pflug & Lundquist, 2020; Revuelto et al., 2014). Because these snowpack patterns repeat on an annual basis, high-resolution snow depth datasets in combination of increasingly sophisticated and ubiquitous terrain, vegetation, and soil property datasets are well suited to improve characterization of the role of fixed physical controls via data intensive methods (e.g., generalized linear or additive models; ensembles of regression trees: random forests or boosted regression trees) that have been used for many purposes in hydrology and ecology (Booker and Woods, 2014; Cutler et al., 2007; He et al., 2016; Tinkham et al., 2014; Peters et al., 2007). One such spatial modeling technique that has not been used to study snow depth patterns is Maximum Entropy (MaxEnt) framework. The MaxEnt in combination with high-resolution remote sensing techniques has the potential to characterize the role of multiple physical variables simultaneously on snow depth spatial variability as well as their relative importance.

MaxEnt is a machine learning approach that uses the spatial location of focal features and predictor variables to extrapolate these features across a landscape where those predictor variables are present (Baldwin, 2009; Phillips et al., 2004; 2006; Phillips & Dudík, 2008). In the ecological science community, the MaxEnt framework has been widely used for a species distribution modelling, with over 1000 published applications between 2006 to 2013 (Elith et al., 2006; Phillips & Dudík, 2008; Merow et al., 2013, Algeo et al., 2017). Using the MaxEnt model, ecologists predicted habitat suitability of animal and plant species using related spatial-environmental factors as predictor variables (Dudik et al., 2007). The principle of the MaxEnt model originates in information theory (Jaynes, 1957), but its application has been expanded to various disciplines, such as archaeology (Howey et al., 2016, 2020), plant distribution (McMichael et al., 2014), and soil and drought (Palace et al., 2017). MaxEnt has been applied in hydrology to a range of problems (Singh 1997; Fischer et al., 2020; Westhoff et al., 2014) including to constrain hydrologic model parameters (Westhoff and Zehe, 2012), map groundwater (Rahmati et al. 2016), evaluate effect soil structure on hydrologic fluxes via preferential flow paths (Zehe et al., 2010) and characterize land-surface hydrology (Wang and Bras, 2011; Djebou and Singh, 2015). Importantly, the MaxEnt framework provides valuable information about variable importance with a model reliability that dominates the overall contribution for developing the MaxEnt model. While entropy-based methods have advantages over traditional statistical methods (Mishra and Coulibaly, 2009), research regarding the use of entropy theory for understanding snow variability across a landscape is limited to snow monitoring network design (Keum et al., 2018) Among the diverse network design methods, the entropy-based methods have emerged as promising alternatives to traditional statistical methods (Mishra and Coulibaly, 2009).

The main objective of this study is to identify physical drivers controlling spatial variability of snow depth focusing on shallow, ephemeral snowpacks using information from a UAS-based lidar platform. MaxEnt modeling efforts are used to evaluate the relative importance of terrain, plant functional type, and soil variables in identifying the location of the shallowest and deepest snowpack as well as the consistency of snow depth patterns. This paper is organized as follows. Section 2 provides the study site information with general land characteristics and weather conditions with several field photos. Section 3 describes the datasets including the UAS lidar snow depth and physical static variables. The description of the MaxEnt model is included Section 3.3. Section 4 details the results of spatial patterns of the lidar snow depth from two flights measured in different winters and the dominant drivers contributing the spatial variability of snow depth. Section 5 offers a discussion about the similarities, differences, and new findings in the results with respect to previous studies. Conclusions and future perspectives are drawn in section 6.

2. Study site

This study was conducted at the University of New Hampshire Thompson Farm Research Station in southeast New Hampshire, United States (N 43.10892°, W 70.94853°, 35 m above sea level), which was chosen for its mixed hardwood forest and open field land covers (Perron et al. 2004; Burakowski et al., 2015; Burakowski et al., 2018; Sanders-DeMott et al. 2020) that are characteristic of the region (**Figure 1**). Thompson Farm has an area of 0.83 km^2 and little topographic relief (18 to 36 m ASL) (Perron et al., 2004). The agricultural fields are actively managed for pasture grass. The mixed deciduous and coniferous forest is composed primarily of white pine (*Pinus strobus*), northern red oak (*Quercus rubra*), red maple (Acer rubrum), shagbark hickory (*Carya ovata*), and white oak (*Quercus alba*) (Perron et al., 2004). There are two “wood roads” that run north-south through the pasture and into the western forest section. The winter climate at Thompson Farm is characterized by cold, maritime winter climate with a mean winter air temperature of -3.0°C, snowfall of 114 cm (NH State Climate Office, 2014), and three weeks to over three months of days with snow cover (Burakowski and Hamilton, 2020). Snow depth can range from a trace up to 94 cm and typical snow density ranges from 100 to 400 kg/m^3 (Burakowski et al. 2013).

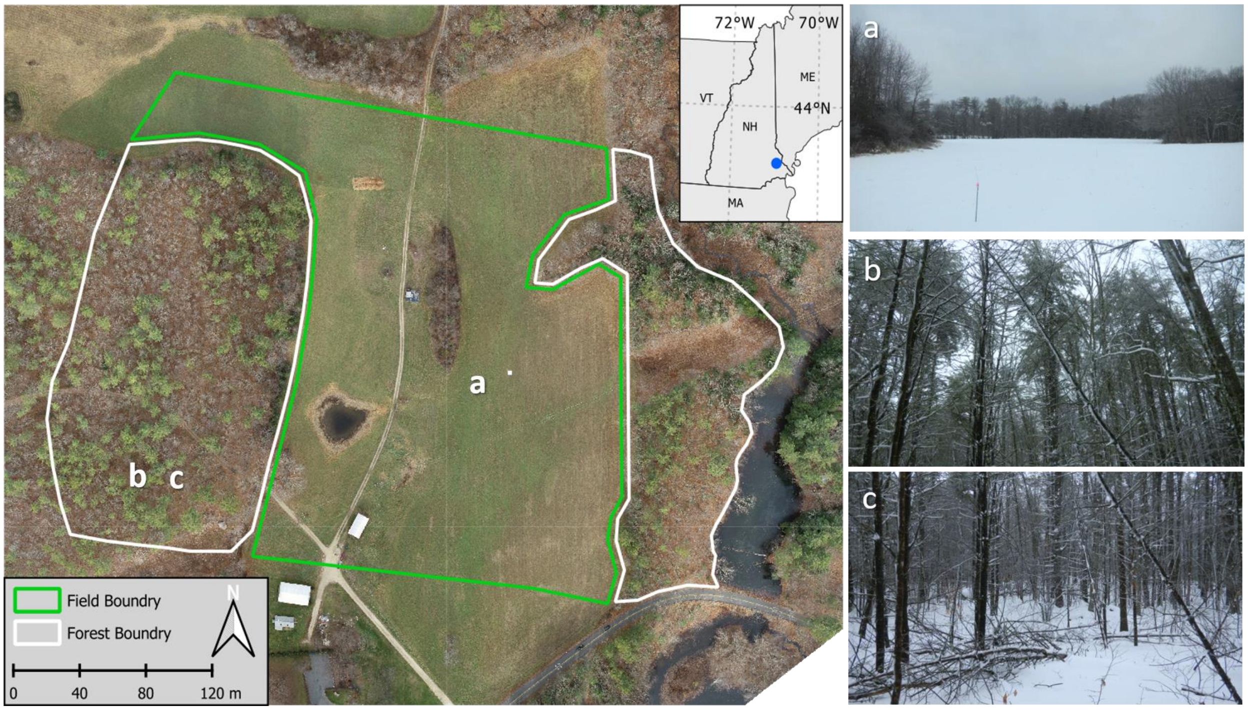

Figure 1. Study location with a leaf-off image of Thompson Farm, Durham, New Hampshire, United States (left) with examples of photos showing the field and forest conditions (right) in December 2019 (Snow-on image with flight lines is provided in **Figure S1**).

3. Datasets and Methods

3.1 UAS lidar snow depth

UAS lidar surveys were conducted at the Thompson Farm Research Station during two consecutive winter seasons. This study compares two lidar derived snow depth products that represent the distribution of snow depth at a spatial resolution of one meter. Snow surface elevations were collected on January 23rd, 2019 and December 4th, 2019. The respective bare earth baseline elevations were collected following snowmelt on April 11th, 2019 and March 18th, 2020. The total area surveyed was approximately 0.11 km^2, of which 0.7 km^2 was open field and 0.4 km^2 was mixed deciduous (dormant) and coniferous forest.

A heavy lift quadcopter manufactured by UAV-America was used to carry lightweight and inexpensive Lidar and GNSS-inertial sensors. The Lidar sensor used was the Velodyne VLP-16. The VLP-16 has 16 independent infrared lasers that rotate 360 degrees along the horizontal axis and are evenly spaced from -15 to +15 degrees along the vertical axis. The sensor was configured to only collect the strongest return per laser pulse, resulting in approximately 300,000 laser shots per second. Lidar distance observations were georeferenced using the UAS trajectory and attitude observed with the Applanix APX-15 IMU/GPS. The APX-15 uses a high performance GNSS receiver that achieves a positional accuracy of 2-5 cm following post-processing. Post-processing was accomplished using the POSPac UAS software package and a nearby continuously operating reference station (CORS) GNSS base station. Micro electromechanical systems (MEMS) sensors are also used by the APX-15 to capture UAS attitude with uncertainties of 0.025-degree roll and pitch, and 0.08-degree true heading. The APX-15 collects positional and attitude observations at a rate of 200 Hz, enabling the high frequency Lidar observations to be accurately georeferenced. UAS flights were conducted at an altitude of 81 meters. This altitude was selected to achieve maximum swath width (~150m) while remaining in the operational range limits of the VLP-16 Lidar sensor. A lawn mower flight plan with a targeted swath overlap of 40% was used on the January 23rd, 2019 survey and the respective baseline. In an effort to achieve a denser point cloud, a crossed flight plan with a target swath overlap of 40% between parallel flight lines was used for the December 4th, 2020 survey and the respective baseline (**Figure 1**). Similar point densities were achieved between the two flights. A flight speed of 7 m/s was used for both flights.

Point Clouds were filtered to remove all non-ground laser returns using a progressive morphological filter as part of the R package LidR. Classified lidar returns were then averaged over a one-meter grid to create digital elevation models (DEMs) for the bare earth and snow surfaces. Snow depth maps were constructed by simply subtracting the snow-on DEM from the bare-earth DEM.

3.2 Physical variables

Topographic and soil variables were investigated as potential physical drivers of field scale snow depth spatial variability. Variables included in this study were plant functional type, roughness, slope, shading, aspect, inter-pixel variability of lidar returns (STD), topographic compound index (TCI), saturated hydraulic conductivity (K_{sat}), and soil organic matter (**Figure 2**). Mapped at a one-meter scale, all physical variables are derived from our UAS observations except the two soil variables. The soil variables, saturated hydraulic conductivity and organic matter of the soil at depth of 0–5 cm, were obtained from Probabilistic Remapping of SSURGO (POLARIS) soil property maps (30-m spatial resolution; Chaney et al., 2016; 2019).

The topographic variables, percent slope and aspect, were calculated using Horn's method (Horn, 1981). Surface roughness was calculated as the largest intra-cell difference of a central pixel and its eight surrounding cells. Inter-pixel variability of lidar returns (STD) is the standard deviation of the lidar returns within each pixel and is a measure of the small-scale surface roughness. Topographic compound index (TCI), also known as or topographic wetness index, is used to estimate the surface water that might accumulate across a landscape (Sørensen et al., 2006; Howey et al., 2016). This metric is computed as $A/\tan B$, the cumulative upslope region (A) that drains through a specific point along a contour path (B). Total shading represents the number of hours from 7 am to 5 pm that a pixel was in the shade on the survey date and was calculated using the unfiltered UAS-lidar DTM and the incidence angle of the sun on the survey date. Binary shadow maps (shadow or no-shadow) were made for each hour from 7 am to 5 pm then merged to count the number of hours that a pixel was in the shade. To characterise the local variability of snow depth (~10 m), the local gradient of the snow surfaces and their respective baselines (snow-off) were calculated using image convolution through a 9 x 9 pixel moving window. The horizontal gradient within the moving window was calculated as the difference between the mean pixel values to the left of the center column and the mean pixel values to the right of the center column. The vertical gradient within the moving window was calculated as the difference between the mean pixel values above the center row and the mean pixel values below the center row. The total local gradient (LG) was then calculated by summing the gradient components as follows:

$$\text{Total local gradient} = \sqrt{Horizontal\ gradient^2 + Vertical\ gradient^2} \tag{1}$$

At least 50% of the pixels within each window had to have snow depth data (e.g., percentage of pixels with data to the left of the center column). If this condition was not met for any portion of the window used to calculate the gradient components, a value of not available (NA) was recorded for the total gradient at this location.

3.3 Maximum Entropy (MaxEnt) model

To identify physical variables that control the spatial variations of the snow depth estimated from a UAS lidar system, we used the MaxEnt framework in the context of a shallow, ephemeral snowpack. The nine topographical and soil static variables (from section 3.2) were used to develop probability maps of snow distribution (shallow or deep) along with examining the importance of the specific variables mentioned above (**Figure 2**). The important variables identified from the MaxEnt models that predict the suitability of the area for relatively deep or shallow snow depths can be considered as a proxy for physical drivers to generate spatial variability of snowpack. There are two types of variable importance values from the MaxEnt framework, percent contribution and permutation importance. The percent contribution values are heuristically defined. They depend on the particular algorithm path that the MaxEnt model uses to obtain the optimal solution. The permutation importance depends on the final MaxEnt model, not the path. This importance for each input variable is determined by randomly permuting the values of the variable among the training points (See details in Phillips, 2006). Percent contribution is presented in the body of the paper, and permutation importance results are included in the Supporting Information.

To check the reliability of the MaxEnt models, area under the receiver-operator curve (AUC) is used in this study, which indicates the predictive capacity of the model (Merow et al., 2013). AUC, which varies from 0 to 1, is interpreted as the probability that a randomly chosen presence location is ranked higher than a randomly chosen absence point. An AUC value of 0.5 is the same as a random guess of presence/absence. The closer an AUC value is to 1, the more reliable the predictions from the MaxEnt model. A model with an AUC over 0.75 is often considered to accurately estimate sample data (Phillip and Dudík, 2008).

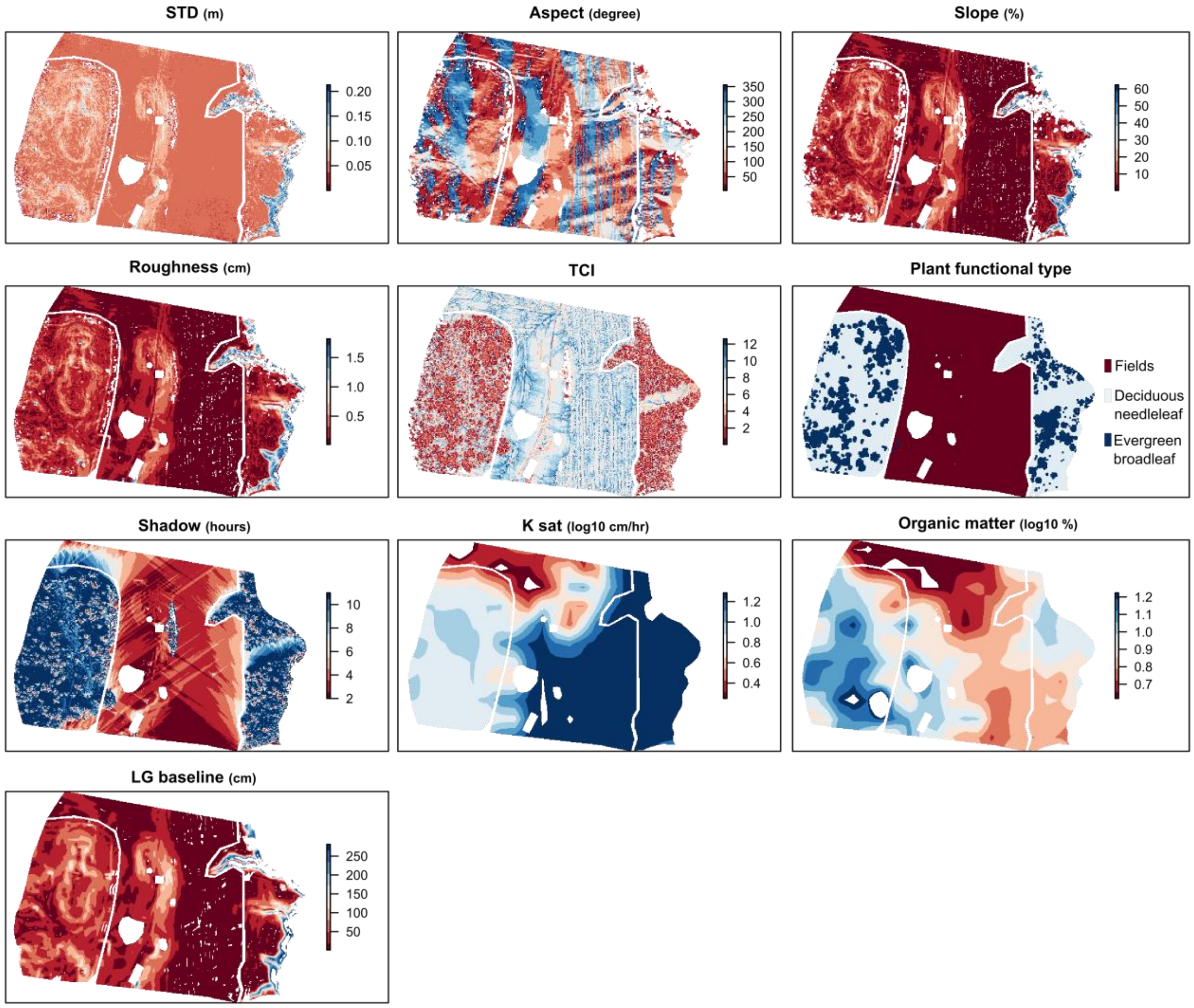

Figure 2. Spatial maps of the nine topographic and soil variables plus the local gradient of baseline used as input variables for the Maximum Entropy model

4. Results

4.1 Relationship among physical variables

Before conducting the MaxEnt model analysis to identify physical drivers controlling spatial variability of snow depth, cross-correlation matrices among the physical input variables were calculated for (1) landscape scale (fields and forest combined), (2) fields, and (3) forest. **Figure 3** shows the cross-correlation matrices with the Pearson correlation coefficients (R-values) with different colors. For all three areas, roughness is strongly correlated with slope (R =

0.69, 0.95, and 0.69 for landscape scale, fields, and forest, respectively). While slope and roughness are moderately correlated with standard deviation of lidar returns (STD; R: 0.63 for both) in fields, they are less strongly correlated (R = 0.39 and 0.34) in forest areas. For the fields, there is also a strong correlation (R = 0.65) between saturated hydraulic conductivity (K_{sat}) and organic matter of soils.

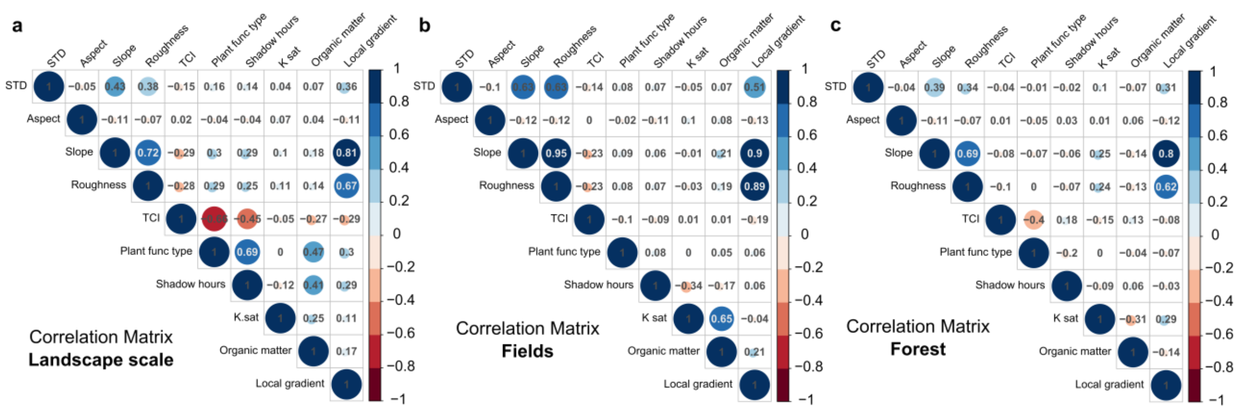

Figure 3. Cross-correlation matrices for landscape scale, fields, and forest based on the boundaries from Figure 1

4.2 Spatial patterns of snow depth

The UAS lidar-based snow depths, mapped by subtracting snow-off DTMs from snow-on DTMs, reveal a thin snow pack ranging from less than 2 cm to over 21 cm in January 2019 (mean: 9.4 cm; standard deviation: 9.7 cm) and depths exceeding 41 cm in December 2019 (mean: 26.9 cm; standard deviation: 15.2 cm) (**Figure 4** and **Table 1**). As compared to in situ magnaprobe (Sturm and Holmgren, 2018) snow depth measurements, the lidar snow depth measurements had mean absolute differences (MAD) and root mean squared difference (RMSD) values of 0.96 cm and 1.22 cm, respectively, in the open field, and the MAD and RMSD values were 9.6 cm and 10.5 cm, respectively, in the forest in January 2019 (see details in Jacobs et al., 2020). The lidar snow depth map in December 2019 had MAD and RMSD of 1.6 cm and 2.0 cm, respectively, in the open field and MAD and RMSD of 3.0 cm and 3.9 cm, respectively, in the forest.

The shallower snow depths (lower 30%) were 6.4 cm and 24 cm and deeper snow depths (higher than 70%) for each map) were 12 cm and 29 cm in January and December 2019, respectively. Despite having different magnitudes of snow depth between the two dates, there were similar spatial patterns. Deeper snow depth values (blue) existed in the fields and shallower snow depths (red) in forest. Compared to the forest snowpack, the field snow depth had relatively high spatial variability and less coherent patterns. In the field, the deeper snow is in the northeast areas in January. However, in December, the deeper snow occurred in the middle and east areas. A shallow and spatially consistent snowpack occurred in forest areas. In the deciduous forest type, the snow depth was consistently higher than that in coniferous forest, especially in the east forest (see the plant functional type map in **Figure 2**). The shallowest snowpack was found in coniferous forest type.

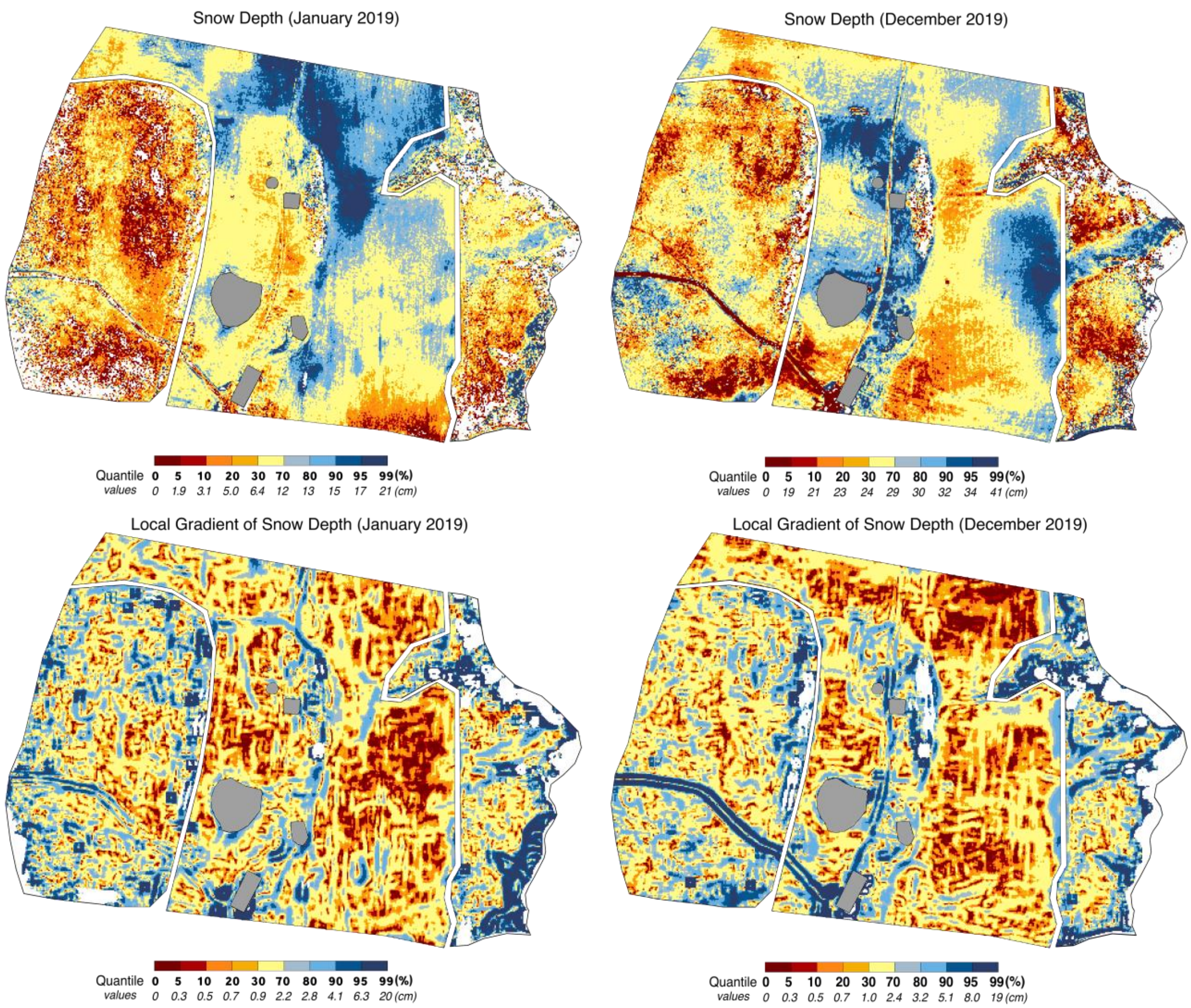

Figure 4. 1-m gridded unpiloted aerial system (UAS) Lidar-based snow depth maps (top panel) and their local gradient maps (bottom panel) in January (left) and December 2019 (right side). To emphasize the

spatial distribution of shallower (lower) or deeper (higher) values of snow depth (local gradient), the color bars are divided by quantile values (0, 5, 10, 20, 30, 70, 80, 90, 95, and 99%) for each map.

Likewise, spatially coherent patterns of the local gradients of snow depth are readily discernible between the two UAS surveys (**Figure 4**). Lower local gradient values (red), indicating a relatively consistent snow depth, existed in the east fields. Higher gradients (blue) were found in the field to forest transitions and roads. In the forest areas, the lower local gradients generally appeared in coniferous forest. High local gradients are consistently found at the forest edge.

Table 1. Summary of snow depth and local gradient of snow depth in January and December 2019

	Snow depth (cm)						Local gradient of snow depth (cm)					
Areas	January 2019			December 2019			January 2019			December 2019		
	Mean	Std	99%	Mean	Std	99%	Mean	Std	99%	Mean	Std	99%
Landscape	9.4	9.7	21.7	26.9	15.2	40.9	2.7	10.8	19.8	2.7	6.7	19.3
Fields	11	3.8	19.9	27.8	6.8	38.2	1.6	4.1	8.1	2	5.4	14.1
Forest	7.2	13.8	27.4	25.8	21.1	46.8	3.9	15.3	35	3.6	7.8	21.5

4.3 Physical drivers contributing spatial variability of snow depth

To determine the most relevant physical drivers that contribute to the spatial variability of snow depth, the relative importance of the input variables from the MaxEnt model with different thresholds was quantified. **Figure 5** shows relative contribution of the nine input variables from each MaxEnt run using the shallow and deep snow depth values within thresholds. Larger percentages indicate those variables that play a greater role in predicting the suitability of shallow or deeper snow depth.

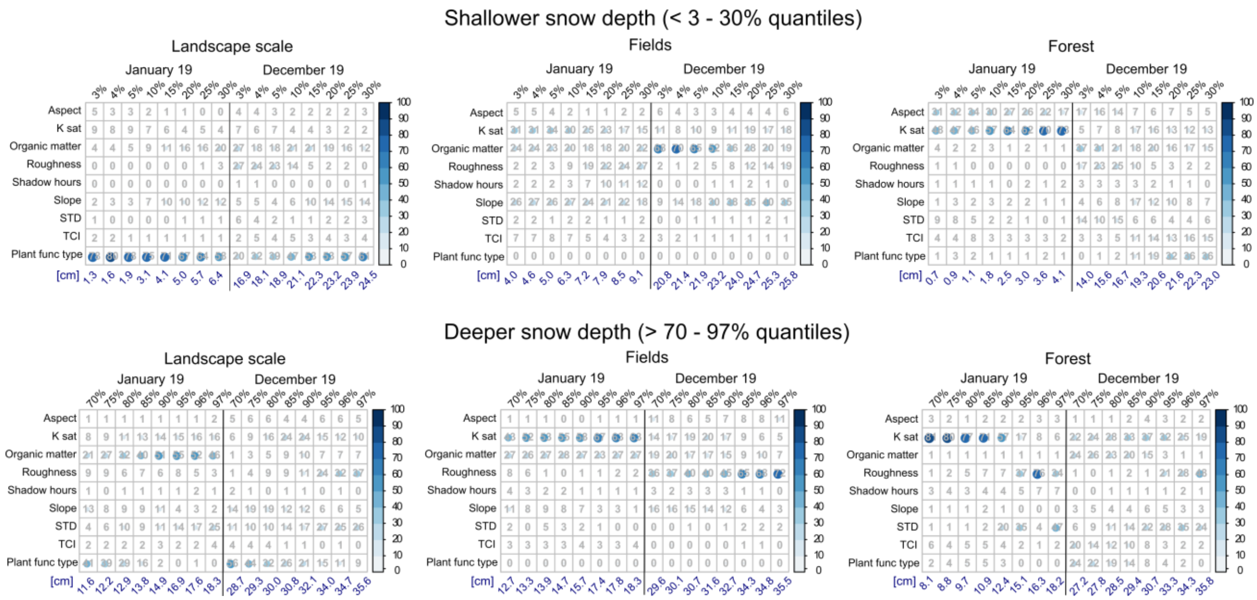

Figure 5. Variable importance from the MaxEnt models for shallower and deeper snow depth observed in January (left) and December 2019 (right side of each subfigure). Shallower or deeper snow depth is determined by thresholds. Shallower snow depth is defined as less than 3% (extremely shallow) to 30% quantiles (moderately shallow) of the entire snow depth values for the three areas, landscape, fields, and forest, respectively. Deeper snow depth values are from larger than 97% (extremely deep) to 70% quantiles (moderately deep). Permutation importance values for the snow depth are also provided in Supporting information (**Figure S2**).

For shallow snow depths (top panels), plant functional type is the most important variable in the landscape scale, especially in the January snow depths, which were shallower than the snow depths from December 2019. For the snow depths in December 2019, soil organic matter and roughness contribute somewhat (e.g., both are 27% for the lowest 3% quantile of snow depth). In the fields, soil variables, organic matter and K_{sat}, and slope are generally important. The contribution of soil organic matter to the shallow snow depths in December 2019 is very strong, ranging up to 70%. In the forest, it seems that different variables influence the shallow snowpack for the two study snowpacks. While K_{sat} and aspect are clearly important to identify shallow snow depth in January 2019 as compared to other variables, there are no dominant variables in December 2019. Organic matter (21 to 37%) and roughness (17 to 23%) are somewhat important for extremely shallow snow depths (less than 3 to 5% quantiles).

For deep snow depths (bottom panels), different variables contribute to snow depth for the two study snowpacks. While organic matter is the dominant control in January, landscape scale, roughness and STD are more important in December. In the fields, K_{sat} and organic matter indicate locations of deep snow in January, but roughness is the most important variable in

December. In the forest, the variable contributions differ by snowpack. For the deepest snow depth (95 to 97% quantiles), roughness (and STD) is important but the contributions of K_{sat} and organic matter gradually increase when the threshold for deep snow is decreased.

In summary, plant functional type is an important explanatory variable for mixed vegetation areas, especially in predicting the shallow snow depth. Soil variables, organic matter and K_{sat}, contribute to both shallow and deep snowpacks. Roughness and STD are also important particularly for the snow depth in December 2019 rather than in January 2019. Contrary to expectations, shadow hours, aspect, and TCI had limited ability to identify the relatively shallow or deep snow depth in the MaxEnt framework.

Predicted suitability maps of shallower or deeper snow depth can be estimated from the MaxEnt models developed for target ranges. Based on the training points with input variables, the MaxEnt model provides potential locations with suitability where the range of snow depth likely exists. For example, **Figure 6** includes predicted suitability maps for the locations where the snow depth is less than the 5% quantile and greater than the 95% snow depth quantile for the two snowpacks. These maps are the combination of the two maps developed by the MaxEnt models for fields and forest, respectively. In January, locations with high predicted suitability (dark red) for shallow snowpack correspond to locations with shallow snow depth (e.g., west forest, south fields, and central fields near ponds; see **Figure 4**). In December, distributions with high suitability also agreed fairly well with the shallow values from the snow depth map (e.g., southwest fields and east forest). For the 95% snow depth quantile, predicted maps with high suitability values captured areas where deep snow depth exists (e.g., northeast fields in January 2019, central fields near the small buildings in December 2019, and east forest in both months).

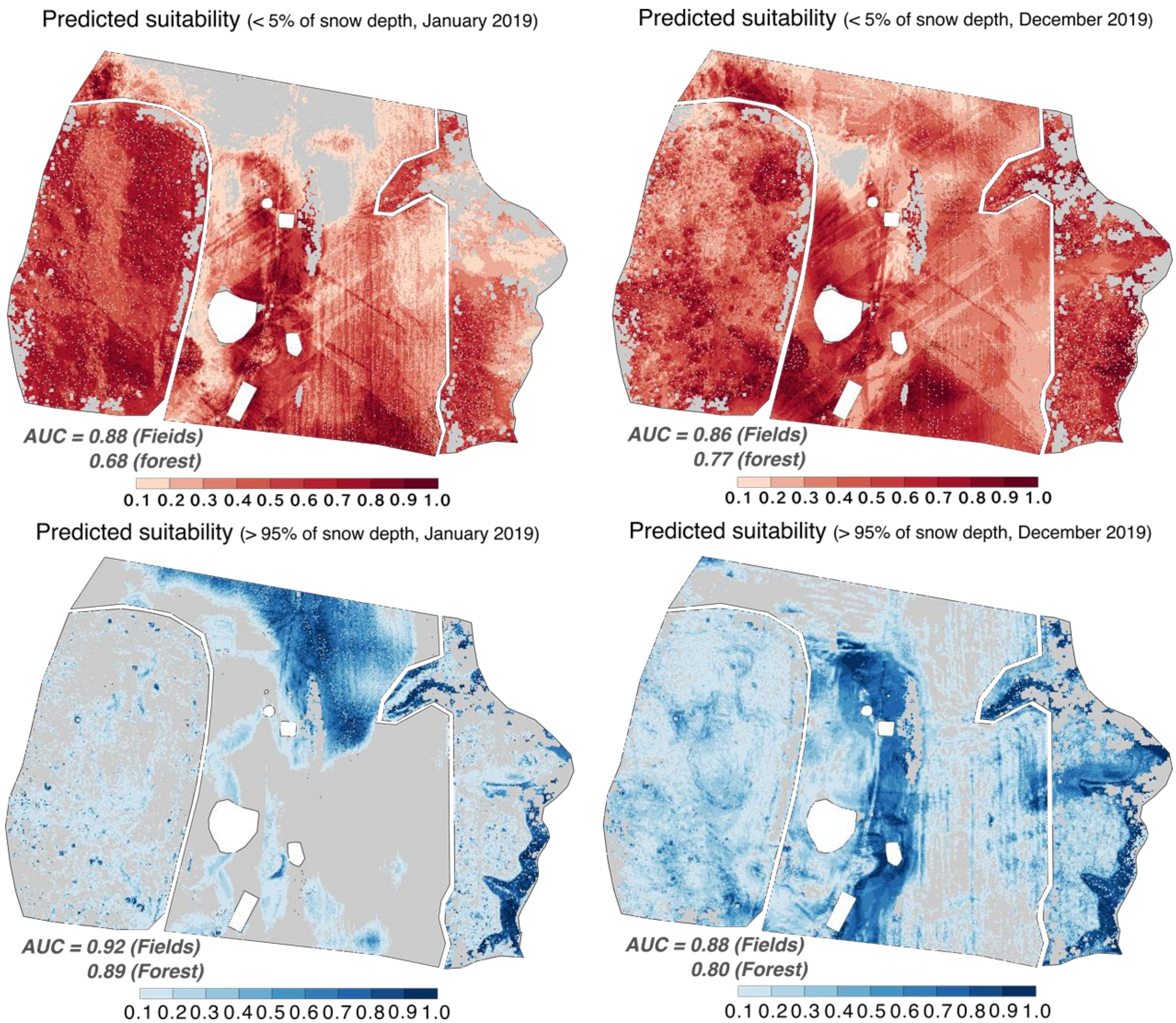

Figure 6. Predicted suitability maps of shallower (< 5 % quantile; top panel) and deeper (> 95 % quantile; bottom panel) snow depth from the Maximum Entropy (MaxEnt) models in January (left) and December 2019 (right side), separately.

In an effort to better discern the effect of the soil variables on the reliability of the MaxEnt model, AUC values are compared for models that include and exclude soil variables (**Figure 5**). The AUC values from the MaxEnt models for the shallowest (3 to 5%) and deepest snow depths (95 to 97% quantiles) are higher than the moderate snow depths (10 to 30% and 70 to 95%). For both shallow and deep snow depths, the MaxEnt models with soil variables have higher AUC values than the MaxEnt models without soil variables. This tendency is more apparent in the field than the forest. For fields with shallow snow depth, AUC values with soil variables range from 0.86 to 0.92 for the 3 to 5% snow depth quantiles, while the values without soil variables range from 0.76 to 0.83. For fields with a deep snow pack, there is a more modest influence. The AUC values with soil variables for the 95 to 97% quantiles range from 0.86 to 0.93, while the values without soil variables are range from 0.79 to 0.87.

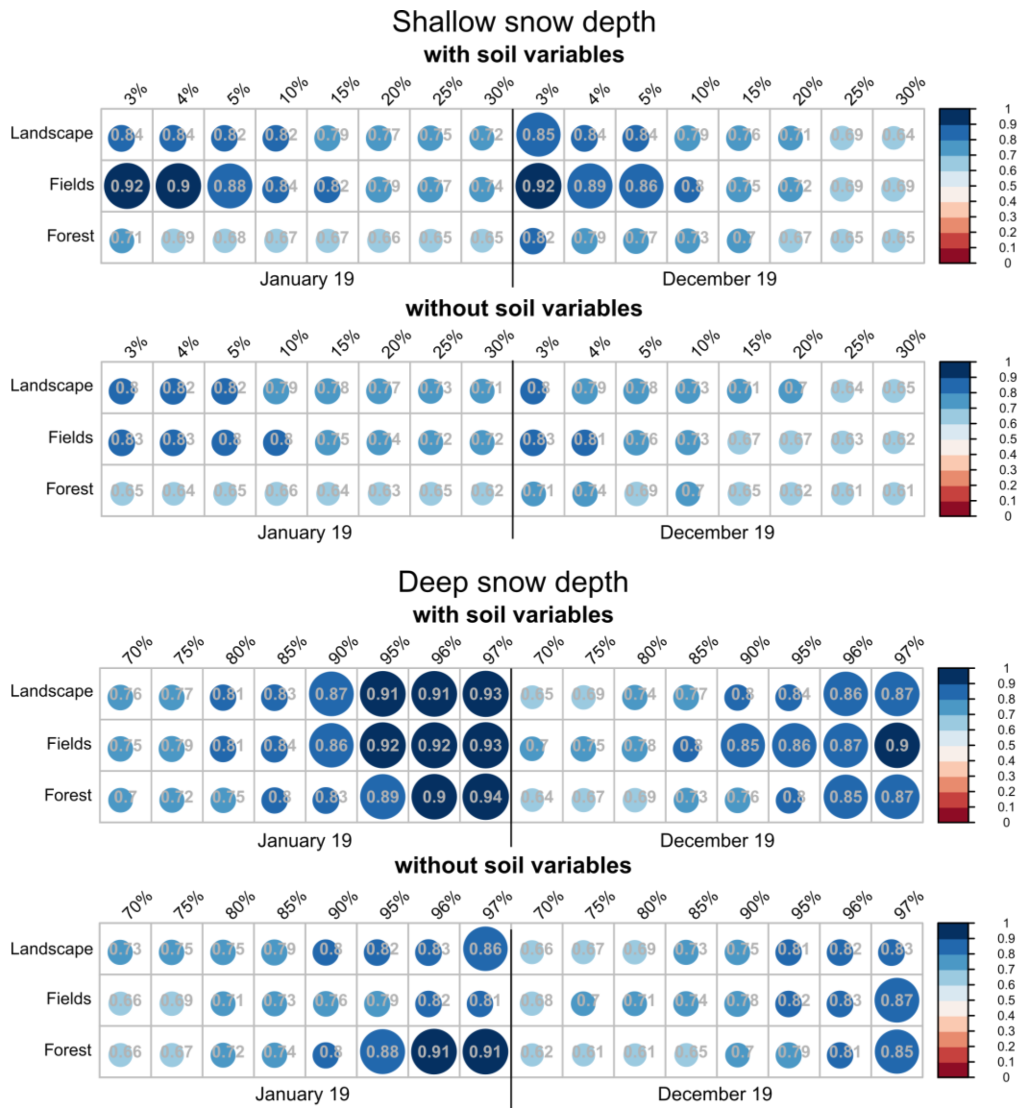

Figure 5. Comparison of the Area Under the receiver-operator Curve (AUC) values of the MaxEnt models with and without soil variables (organic matter and saturated hydraulic conductivity) for shallow and deep snow depths observed in January and December 2019.

4.4 Localized variability of snow depth

The relative contributions of the static variables on the snow depth local gradients were computed in the MaxEnt framework for locations having lower (less than 3 to 30%) and higher local gradients (greater than 7% to 97%) (**Figure 6**). For this analysis, the static variable included the nine input variables previously used as well as the local gradient mapped during the baseline (snow-off) flight. Variables with larger percentages indicate that the input variables play a greater role in predicting the local gradients and typically improving the MaxEnt's reliability. For low local gradients of snow depth, implying locally homogeneous snowpack conditions within 10 m (top panels), plant functional type was the most important variable (32 – 49%) for landscape scale, especially in the shallower snow depth map from January. Roughness and the baseline local gradient were of secondary importance in January and December, respectively. Roughness contributed 24% and baseline local gradient contributed 23% for the less than 3% quantile of local gradients. In the fields, there were clear differences in important variables between the two snowpacks. While soil variables, organic matter and K_{sat}, and roughness were important for January, the baseline's local gradient was the strongest contributor for December. In the forest, there were no dominant variables, except for the baseline's local gradient for January. Aspect, shadow hours, STD, and TCI did not play a role in the location of low local gradients for the overall site, nor for the field and forest areas.

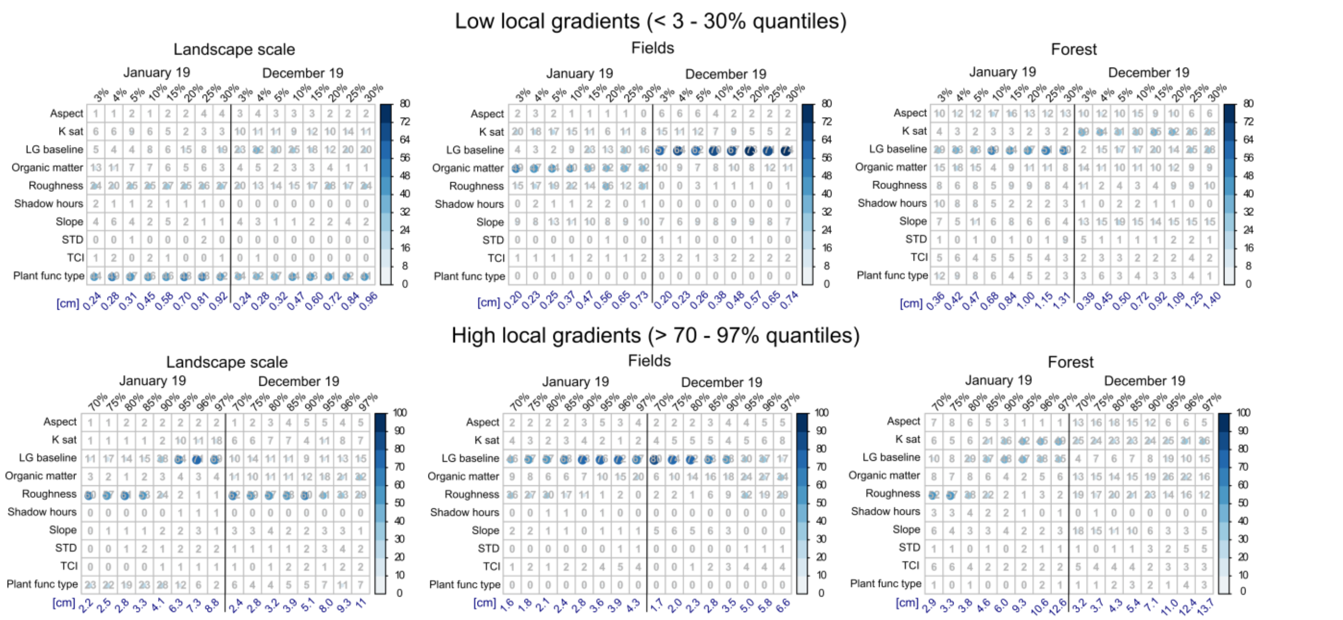

Figure 6. Variable importance from the MaxEnt models for low (top) and high (bottom panel) local gradients of snow depth observed in January (left) and December 2019 (right side of each subfigure). Low or high local gradients of snow depth are determined by thresholds. Low local gradient is defined as less than 3% (extremely low) to 30% quantiles (moderately low) of the entire local gradient values for the three areas, landscape, fields, and forest, respectively. High local gradient values are from larger than 97% (extremely high) to 70% quantiles (moderately high). Permutation importance for the local gradients are also provided in Supporting information (**Figure S3**).

For high local gradients of snow depth (bottom panels), roughness and the baseline local gradient are important for identifying landscape scale transitions. For the January snowpack, the contributing percentage of the baseline's local gradient was around 70% for the extremely high local gradients (95 to 97% quantiles). The contribution of the baseline local gradient decreased with decreasing thresholds, and roughness's contribution increased indicating a transition between the two highly correlated variables. In fields, the baseline local gradient was the dominant control and contributed up to 80%. Organic matter was also somewhat important (up to 20 to 34%) for the highest local gradient of snow depth (higher than 95% quantiles). In the forest, while there were no dominant variables as compared to fields or landscape scale, for January, K_{sat} and baseline's local gradient were important (49% and 36%, respectively). Contribution of roughness gradually increases with decreasing the quantiles (particularly from 70 to 85% quantiles).

In summary, plant functional type is valuable for predicting the low local gradients of snowpack at the landscape scale. Within a single plant functional type, the baseline's local gradient and roughness control the locations of both the low and high local gradients of snow depth. Soil variables also contribute modestly to identifying spatial variability in localized snowpack. Contrary to our expectations, shadow hours, aspect, and TCI had marginal contributions for localized snowpack variations at the 10 m scale using the MaxEnt framework.

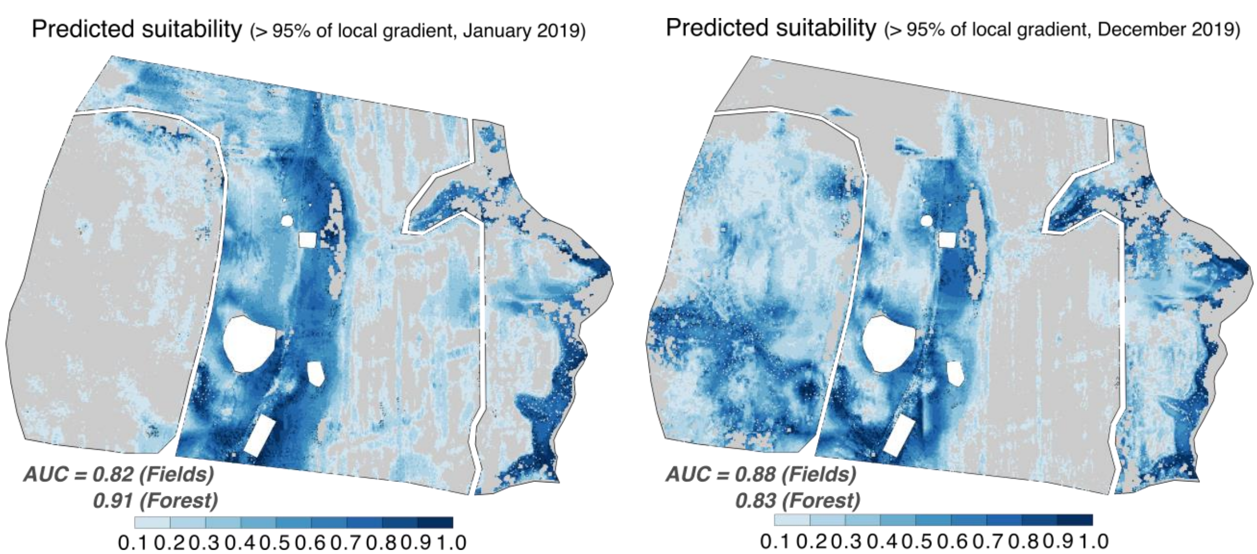

Figure 7. Predicted suitability maps of high local gradient of snow depth maps (> 95 % quantile) from the Maximum Entropy (MaxEnt) modelling framework on January (left) and December 2019 (right side).

In contrast with predicted suitability maps of snow depth, two predicted suitability maps of high local gradients have relatively similar spatial patterns for the two snowpacks, except for west forest (**Figure 7**). Because the baseline's local gradient and roughness were the dominant controls needed to predict the local gradients of snowpack, the spatial distributions of baseline's local gradient and roughness are reflected in the predicted maps (compare to the input variable maps in **Figure 2**).

5. Discussion

5.1 Physical drivers: Comparison with previous findings

Static features such as topography and vegetation rather than local meteorology and precipitation patterns typically control snow distribution at the local scale. There are numerous studies, which attempt to characterize spatial snow structures and to identify physical characteristics affecting the spatial characteristics of snowpack. Bloschl and Kirnbauer (1992) investigated the relationship between spatial snow patterns and terrain attributes (e.g., elevation and slope) in a mountainous area in the Austrian Alps. They found no dominant relationship to terrain parameters with spatial snow depth. Lapen and Martz (1996) found that spatial patterns of snow depth are related to the terrain attributes that define sheltering by topographic obstacles, indicating that drifting is a critical process in the prairie environment. Mott et al. (2011) mentioned that the driving force for the drifting processes is the air flow near the surface layer, which is partially shaped by the local terrain. Our results have similar findings in that there were clear differences in snow depth within the fields (e.g., east versus west fields) and transitional areas between fields and forest. Currier and Lundquist (2018) also found large differences in snow depth for the forest-edge classifications in the western United States.

Soil properties are considered to be a potential feature that can affect spatial variability of snowpack, yet few studies have investigated how important soil properties are to inform spatial structure of snow depth as compared to other terrain characteristics. Shook et al. (1993) analyzed area-frequency relationships of snow and soil patches at different stages during the melting season in prairie and alpine environments. They found that snow and soil patches are fractals, and their size distribution is predictable, implying that soil properties may potentially influence such behaviour. Redding and Devito (2011) showed differences in the timing of snow disappearance between two sites with different soil types. They found that mean snowmelt rates at sites with sand soils were quicker than those at sites with loam soils. However, they could not conduct significance tests due to the limited measurements from the loam soils. Our findings indicate that soil properties, organic matter and hydraulic conductivity, are more important than shadow hours, aspect, STD, and for modelling spatial distribution of snow depth, which is probably because soil properties, especially soil organic matter, impact soil thermal conductivity (Abu-Hamdeh and Reeder, 2000). The thermal conductivity of soil is highly dependent on soil density, mineral type, grain size, and moisture content (Farouki, 1981; Penner, 1970; Parikh et al., 1979). In frozen soils, the thermal conductivity is more sensitive to soil type than non-frozen soils, because the thermal conductivity of ice is more than four times larger than that of liquid water (Penner, 1970). Recently, Zhu et al. (2019) found that soil organic matter was a dominant factor controlling the variability of thermal diffusivity at 200 field sites in the high latitude regions. Our results suggest that spatial differences in soil properties may lead to spatial discrepancy in heat transfer between snowpack and soil surface resulting in enhanced spatial variability of snow depth even at local scales. With large spatial variability of soil temperature (e.g., less than 10 m spatial correlation in fields; Mohanty et al., 1995) and frequent patchy snow in shallow ephemeral snowpacks, the differences in energy transfer between snow and soil surface across areas with different snow depths leads to a heterogeneous distribution of surface temperatures (Mott et al., 2013). Harder et al. (2017) confirmed that local-scale sensible heat advection driven by surface temperature heterogeneity is a main source of energy available for snowmelt. Based on our results that soil properties are an important control on the spatial patterns of shallower and deeper snow depths, future research is needed to address the role that spatially distributed soil properties play in the spatial heterogeneity of energy transfer with snowpack.

5.2 MaxEnt framework compared to traditional analysis

To our knowledge this study is the first to use the MaxEnt model to understand snow distribution measured using a UAS-based lidar. In the natural science community, the MaxEnt model is one of the most popular methods for species distribution and environmental modelling (Elith et al., 2006; Merow et al., 2013). The MaxEnt framework provides accurate information about the degree of importance among the input variables that dominate overall contribution to develop the MaxEnt model with model reliability. For the snow science and hydrology community, this approach can create novel opportunities to identify dominant physical variables and to advance snow and land surface models by leveraging remotely sensed snow observations at multiple scales.

As a traditional method, variogram approaches including fractal analysis have been widely used to understand the spatial scaling patterns of snow depth (or SWE) based on the self-similarity of properties over multiple scales. Deems et al. (2006) conducted a variogram analysis of snow depth, topography, and vegetation topography data sets from three 1-km^2 study areas using an airborne-based lidar system. They found the existence of two distinct scale areas from the snow depth and vegetation topography data sets, separated by a scale break that varies between 15 m and 40 m for snow depth, and between 31 m and 56 m for vegetation topography (similar to the results from Arnold and Rees, 2003). Trujillo et al. (2007) also attempted to determine whether the spatial distribution of snow depth has scale invariance, and the role of physical drivers including vegetation, topography, and winds in such behaviour. Using fractal analysis, Schirmer and Lehning (2011) investigated seasonal and spatial changes in scaling behaviour of snow depth. They found that the scale break gradually increases throughout the snow accumulation season indicating that roughness of the terrain surface buried by snow may control the scaling behaviour.

Even though the variogram-type analyses have provided explicit information to characterize the spatial structure of snowpack, limited information is available to determine the relative importance among various physical characteristics related to the formation of spatial structure of snow depth. Deems et al. (2006) speculated that the length of the scale break might be due to the overall terrain relief, and that the process change revealed by the breaks in the variograms of the vegetation topography potentially influences the scaling patterns of snow depth. In Trujillo et al. (2007)'s results, none of the breaks in the slope of the log-log plots between snow depth and the corresponding fields of topography and vegetation topography were present, while the break in the scaling behavior was controlled by the vegetation characteristics (e.g. canopy height, canopy-covered area, and distances between trees). Thus, it is expected that the MaxEnt framework with spatially distributed snowpack data supplements the existing approaches by providing various information about dominant predictor variables along with spatially predicted suitability maps.

5.3 UAS lidar snow depth sampling

Reliable spatially distributed high-resolution snowpack measurements are essential to discern physical processes that depend on the snow state. In this study, the UAS-based lidar system provided a unique opportunity to characterize the spatiotemporal variability of snow depth. Lidar observations can provide not only high resolution snow depths, but also map many of the potential physical drivers of field scale snow depth spatial variability. Over the past two decades, lidar techniques have been widely used to measure snow depth over various spatiotemporal scales and resolutions primarily on aircraft or a fixed ground station (see reviews in Deems et al., 2013; López-Moreno et al., 2017). Airborne laser scanning (ALS) is a well-known lidar technique that is currently leveraged by the Airborne Snow Observatory (ASO) (Painter et al., 2016). The key advantage of ALS is the capability to cover large areas (Deems et al., 2013; Harpold et al., 2014; Kirchner et al., 2014). However, the operation of the system is extremely expensive with limited flexibility of deployment. Lidar sensors are not capable of seeing through clouds, therefore Lidar observations from manned aircraft altitudes are only achievable on clear sky days or when cloud altitudes exceed the aircraft altitude. The spatial resolution of ALS systems is also considerably lower as compared to other Lidar platforms. ALS systems report ground return densities between 3 and 6 points/m^2 (Broxton et al., 2019; Kirchner et al., 2014), resulting in observational gaps in dense forested regions (Currier and Lundquist, 2018; Mazzotti et al., 2019). The limited spatial resolution of ALS would pose challenges to discern the physical processes driving the spatial distribution of snow depth at all relevant scales. Terrestrial laser scanning (TLS) employs high frequency Lidar sensors mounted on a tripod at a fixed ground position (Fey et al., 2019; Hojatimalekshah et al., 2020; Prokop, 2008). TLS has the advantage of being relatively low-cost and portable, making repeat observations possible per day. However, this technique has additional uncertainties caused by large view angles and occlusions from trees and hills (Prokop, 2008; Fey and Wichmann, 2017). Also, in order to accurately georeference observations made with a TLS system it is critical that the tripod remains stationary throughout each scan. In deep snowpacks it is often difficult to ensure the TLS system does not settle within the snowpack and shift position while scanning. Extremely high point densities are achievable with TLS systems; however, the spatial extent of a typical TLS survey is considerably smaller as compared to airborne platforms.

UAS-based lidar has been recently utilized for snow depth mapping (Harder et al., 2020; Jacobs et al., 2020). A UAS platform can eliminate many of the drawbacks that arise from ALS and TLS systems. Obscuration from clouds will rarely be an issue because UAS lidar surveys are generally conducted at an altitude below 120 meters. Although spatial coverage is typically greatly reduced in UAS missions relative to other ALS platforms, the aerial perspective and the large sensor swath overlap facilitated by appropriate mission planning and post-processing provides reduced uncertainties in elevation from those that can result from high off-nadir viewing angles and occlusion in other ALS platforms. In the same vein, flight parameters can be readily adjusted to achieve equally dense point clouds over open and forested areas, improving ground finding and resulting in better characterization of vegetation and terrain mapping. For this study, flight speeds were held constant over both fields and forests, which produced lower return density over the forested part of our study site. There is some evidence that vegetation reduces return density due to scattering and absorption (Liu et al., 2020; Jacobs et al., 2020), so reduced flight speeds over vegetation to account for the reduction in returns could improve terrain characterization in these settings.

6. Conclusion

Understanding the spatial variability of snow is valuable for hydrologists and ecologists seeking to predict hydrological processes, species distributions, land-atmosphere interactions. However, identifying dominant physical drivers controlling the spatial structure of snow depth has been challenged due to the lack of the high-resolution snowpack and physical variables with high vertical accuracy as well as limitations in traditional approaches. To overcome this, we first employ the MaxEnt framework with 1-m spatial snow and terrain maps from a UAS-based lidar system to identify physical variables controlling field scale spatial structures of shallow, ephemeral snow depth over open terrain and forests. We found that, among the nine terrain, plant functional type, and soil variables, plant functional type and roughness had important contribution in the MaxEnt framework as needed to predict spatial locations in either deeper or shallower snow depth across the landscape. Soil organic matter and saturated hydraulic conductivity were revealed as important controls on snow depth spatial variations for both fields and forest, suggesting spatial variations in the soil variables under the snowpack can control thermal transfer between soil and snowpack along with near surface atmosphere. Despite the difference in controls and locations of the relatively shallow and deep snowpacks, the transition zones between areas with similar snow depths, as identified using local gradients, were consistent for both dates and well characterized by the underlying local gradients of baseline flights without snow. It is expected that the results will contribute to advancing snow and land surface models by aiding in the parameterization at the sub-grid scale and helping to support the down-scaling of retrieved remotely sensed snow products to characterize field scale conditions.

Data Availability Statement

The UAS snow depth maps with topographic input variables from this study are available for download at [*will add link to data from Hydroshare, currently being setup with an ODC Attribution (ODC-BY) license for access without restrictions*]. POLARIS Soil property data used in this study are available from Chaney et al. (2019), respectively.

Acknowledgments

This study is based upon work supported by the Broad Agency Announcement Program and the U.S. Army Engineer Research and Development Center's Cold Region Research and Engineering Laboratory (ERDC-CRREL) under contract number W913E5-18-C-005. Any opinions, findings, and conclusions or recommendations in this material are those of the author(s) and do not necessarily reflect the views of the Broad Agency Announcement Program and the ERDC-CRREL. The authors are grateful to Christina Herrick for helping data collection and providing valuable comments.

References

Aanderud, Z. T., Jones, S. E., Schoolmaster Jr, D. R., Fierer, N., and Lennon, J. T. (2013). Sensitivity of soil respiration and microbial communities to altered snowfall, *Soil Biology and Biochemistry*, 57, 217-227.

Aase, J. K. and Siddoway, F. H.: Crown-Depth Soil Temperatures and Winter Protection for Winter Wheat Survival1, *Soil Science Society of America Journal*, 43, 1229-1233, 1979.

Abu-Hamdeh, N. H., & Reeder, R. C. (2000). Soil thermal conductivity effects of density, moisture, salt concentration, and organic matter. *Soil science society of America Journal*, 64(4), 1285-1290.

Algeo, T. P., Slate, D., Caron, R. M., Atwood, T., Recuenco, S., Ducey, M. J., ... & Palace, M. (2017). Modeling raccoon (Procyon lotor) habitat connectivity to identify potential corridors for rabies spread. *Tropical medicine and infectious disease*, *2*(3), 44.

Anderton, S. P., White, S. M., & Alvera, B. (2002). Micro-scale spatial variability and the timing of snow melt runoff in a high mountain catchment. *Journal of Hydrology*, *268*(1-4), 158-176.

Arnold, N. S., & Rees, W. G. (2003). Self-similarity in glacier surface characteristics. *Journal of Glaciology*, *49*(167), 547-554.

Baldwin, R. A. (2009). Use of maximum entropy modeling in wildlife research. *Entropy*, *11*(4), 854-866.

Barnett, T. P., Adam, J. C., & Lettenmaier, D. P. (2005). Potential impacts of a warming climate on water availability in snow-dominated regions. *Nature*, *438*(7066), 303-309.

Blöschl, G., & Kirnbauer, R. (1992). An analysis of snow cover patterns in a small alpine catchment. *Hydrological Processes*, *6*(1), 99-109.

Booker, D. J., & Woods, R. A. (2014). Comparing and combining physically-based and empirically-based approaches for estimating the hydrology of ungauged catchments. *Journal of Hydrology*, 508, 227-239.

Broxton, P. D., Van Leeuwen, W. J., & Biederman, J. A. (2019). Improving snow water equivalent maps with machine learning of snow survey and lidar measurements. *Water Resources Research*, *55*(5), 3739-3757.

Burakowski, E., and Hamilton. L., (2020). Are New Hampshire's Winters Warming? Yes, but fewer than half state residents recognize the trend. Regional Issue Brief #61. Carsey School of Public Policy, University of New Hampshire. https://dx.doi.org/10.34051/p/2020.377

Burakowski, E., Tawfik, A., Ouimette, A., Lepine, L., Novick, K., Ollinger, S., ... & Bonan, G. (2018). The role of surface roughness, albedo, and Bowen ratio on ecosystem energy balance in the Eastern United States. *Agricultural and Forest Meteorology*, *249*, 367-376.

Burakowski, E., Wake, C. P., Dibb, J. E., & Stampone, M. (2013). Putting the capital 'A'in CoCoRAHS: an experimental programme to measure albedo using the Community Collaborative Rain, Hail & Snow (CoCoRaHS) Network. *Hydrological Processes*, 27(21), 3024-3034.

Carroll, R. W., Deems, J. S., Niswonger, R., Schumer, R., & Williams, K. H. (2019). The importance of interflow to groundwater recharge in a snowmelt-dominated headwater basin. *Geophysical Research Letters*, 46(11), 5899-5908.

Chaney, N. W., Minasny, B., Herman, J. D., Nauman, T. W., Brungard, C. W., Morgan, C. L., ... & Yimam, Y. (2019). POLARIS soil properties: 30-m probabilistic maps of soil properties over the contiguous United States. *Water Resources Research*, 55(4), 2916-2938.

Chaney, N. W., Wood, E. F., McBratney, A. B., Hempel, J. W., Nauman, T. W., Brungard, C. W., & Odgers, N. P. (2016). POLARIS: A 30-meter probabilistic soil series map of the contiguous United States. *Geoderma*, 274, 54-67.

Cho, E., Jacobs, J. M., & Vuyovich, C. M. (2020). The value of long-term (40 years) airborne gamma radiation SWE record for evaluating three observation-based gridded SWE data sets by seasonal snow and land cover classifications. *Water Resources Research*, 56(1), e2019WR025813.

Clark, M. P., Hendrikx, J., Slater, A. G., Kavetski, D., Anderson, B., Cullen, N. J., ... & Woods, R. A. (2011). Representing spatial variability of snow water equivalent in hydrologic and land-surface models: A review. *Water Resources Research*, *47*(7).

Currier, W. R., & Lundquist, J. D. (2018). Snow depth variability at the forest edge in multiple climates in the western United States. *Water Resources Research*, 54(11), 8756-8773.

Cutler, D. R., Edwards Jr, T. C., Beard, K. H., Cutler, A., Hess, K. T., Gibson, J., & Lawler, J. J. (2007). Random forests for classification in ecology. *Ecology*, 88(11), 2783-2792.

DeBeer, C. M., & Pomeroy, J. W. (2010). Simulation of the snowmelt runoff contributing area in a small alpine basin. *Hydrology and Earth System Sciences*, *14*(7), 1205.

Deems, J. S., Fassnacht, S. R., & Elder, K. J. (2006). Fractal distribution of snow depth from LiDAR data. *Journal of Hydrometeorology*, 7(2), 285-297.

Deems, J. S., Painter, T. H., & Finnegan, D. C. (2013). Lidar measurement of snow depth: a review. *Journal of Glaciology*, *59*(215), 467-479.

Derksen, C., Toose, P., Rees, A., Wang, L., English, M., Walker, A., & Sturm, M. (2010). Development of a tundra-specific snow water equivalent retrieval algorithm for satellite passive microwave data. *Remote Sensing of Environment*, 114(8), 1699–1709. https://doi.org/10.1016/j.rse.2010.02.019

Djebou, D. C. S., & Singh, V. P. (2015). Retrieving vegetation growth patterns from soil moisture, precipitation and temperature using maximum entropy. *Ecological Modelling*, *309*, 10-21.

Dudik M, Phillips S, Schapire R (2007) Maximum entropy density estimation with generalized regularization and an application to species distribution modeling. *Journal of Machine Learning Research*, 8(6):1217–1260.

Earman, S., Campbell, A. R., Phillips, F. M., & Newman, B. D. (2006). Isotopic exchange between snow and atmospheric water vapor: Estimation of the snowmelt component of groundwater recharge in the southwestern United States. *Journal of Geophysical Research: Atmospheres*, *111*(D9).

Essery, R.L., Bunting, P., Hardy, J. Link, T., Marks, D., Melloh, R., Pomeroy, J., Rowlands, A., and Rutter., N. (2008). Radiative transfer modeling of a coniferous canopy characterized by airborne remote sensing. *Journal of Hydrometeorology*, 9: 228–241.

Elith J, et al. (2006) Novel methods improve prediction of species' distributions from occurrence data. *Ecography* (Cop.) 29(2):129–151.

Farouki, O. T. (1981). The thermal properties of soils in cold regions. *Cold Regions Science and Technology*, 5(1), 67-75.

Fey, C., Schattan, P., Helfricht, K., & Schöber, J. (2019). A compilation of multitemporal TLS snow depth distribution maps at the Weisssee snow research site (Kaunertal, Austria). *Water Resources Research*, *55*(6), 5154-5164.

Fey, C., & Wichmann, V. (2017). Long‐range terrestrial laser scanning for geomorphological change detection in alpine terrain–handling uncertainties. *Earth Surface Processes and Landforms*, *42*(5), 789-802.

Fischer, S., Bühler, P., Büttner, U., & Schumann, A. (2020). The use of maximum entropy to increase the informational content of hydrological networks by additional gauges. *Hydrological Sciences Journal*, *65*(13), 2274-2285.

Ge, Y., & Gong, G. (2010). Land surface insulation response to snow depth variability. *Journal of Geophysical Research: Atmospheres*, 115(D8).

Gelfan, A. N., Pomeroy, J. W., & Kuchment, L. S. (2004). Modeling forest cover influences on snow accumulation, sublimation, and melt. *Journal of Hydrometeorology*, *5*(5), 785-803.
Goetz, J., & Brenning, A. (2019). Quantifying uncertainties in snow depth mapping from structure from motion photogrammetry in an alpine area. *Water Resources Research*, *55*(9), 7772-7783.
Gray, D. M., & Male, D. H. (1981). Handbook of snow: Principles, processes, management and use. Toronto: Pergamon Press.
Grayson, R. B., Blöschl, G., Western, A. W., & McMahon, T. A. (2002). Advances in the use of observed spatial patterns of catchment hydrological response. *Advances in Water Resources*, *25*(8-12), 1313-1334.
Groffman, P. M., Driscoll, C. T., Fahey, T. J., Hardy, J. P., Fitzhugh, R. D., & Tierney, G. L. (2001). Colder soils in a warmer world: a snow manipulation study in a northern hardwood forest ecosystem. *Biogeochemistry*, *56*(2), 135-150.
Grünewald, T., and M. Lehning (2011), Altitudinal dependency of snow amounts in two small alpine catchments: Can catchment-wide snow amounts be estimated via single snow or precipitation stations, *Annals of Glaciology*, 52(58), 153–158, doi:10.3189/172756411797252248.
Harder, P., Pomeroy, J. W., & Helgason, W. (2017). Local-scale advection of sensible and latent heat during snowmelt. *Geophysical Research Letters*, 44(19), 9769-9777.
Harder, P., Pomeroy, J. W., & Helgason, W. D. (2020). Improving sub-canopy snow depth mapping with unmanned aerial vehicles: lidar versus structure-from-motion techniques. *The Cryosphere*, 14(6), 1919-1935.
Harpold, A. A., Guo, Q., Molotch, N., Brooks, P. D., Bales, R., Fernandez-Diaz, J. C., ... & Flanagan, J. (2014). LiDAR-derived snowpack data sets from mixed conifer forests across the Western United States. *Water Resources Research*, *50*(3), 2749-2755.
Harpold, A. A., Molotch, N. P., Musselman, K. N., Bales, R. C., Kirchner, P. B., Litvak, M., & Brooks, P. D. (2015). Soil moisture response to snowmelt timing in mixed-conifer subalpine forests. *Hydrological Processes*, 29(12), 2782-2798.
He, X., Chaney, N. W., Schleiss, M., & Sheffield, J. (2016). Spatial downscaling of precipitation using adaptable random forests. *Water Resources Research*, 52(10), 8217-8237.
Henry, H. A. L. (2008). Climate change and soil freezing dynamics: historical trends and projected changes, *Climatic Change*, 87, 421-434.
Hojatimalekshah, A., Uhlmann, Z., Glenn, N. F., Hiemstra, C. A., Tennant, C. J., Graham, J. D., ... & Enterkine, J. (2020). Tree canopy and snow depth relationships at fine scales with terrestrial laser scanning. *The Cryosphere Discussions*, 1-35. https://doi.org/10.5194/tc-2020-277
Horn, B.K.P. (1981). Hill shading and the reflectance map. *Proceedings of the IEEE*, 69(1): 14-47. Doi: 10.1109/PROC.1981.11918.
Howey, M. C., Palace, M. W., & McMichael, C. H. (2016). Geospatial modeling approach to monument construction using Michigan from AD 1000–1600 as a case study. *Proceedings of the National Academy of Sciences*, 113(27), 7443-7448.
Huerta, M.L, Molotch, N.P., and McPhee. J., (2019). Snowfall interception in a deciduous Nothofagus forest and implications for spatial snowpack distribution. *Hydrological Processes*, 33(13): 1818-1834.
Isard, S. A., & Schaetzl, R. J. (1998). Effects of winter weather conditions on soil freezing in southern Michigan. *Physical Geography*, *19*(1), 71-94.

Jacobs, J. M., Hunsaker, A. G., Sullivan, F. B., Palace, M., Burakowski, E. A., Herrick, C., & Cho, E. (2020). Shallow snow depth mapping with unmanned aerial systems lidar observations: A case study in Durham, New Hampshire, United States. *The Cryosphere Discussions*, 1-20.

Jaynes E. T. (1957) Information theory and statistical mechanics. *Physical Review*. 106(4):620–630.

Keum, J., Coulibaly, P., Razavi, T., Tapsoba, D., Gobena, A., Weber, F., & Pietroniro, A. (2018). Application of SNODAS and hydrologic models to enhance entropy-based snow monitoring network design. *Journal of Hydrology*, *561*, 688-701.

Kirchner, P. B., Bales, R. C., Molotch, N. P., Flanagan, J., & Guo, Q. (2014). LiDAR measurement of seasonal snow accumulation along an elevation gradient in the southern Sierra Nevada, California. *Hydrology & Earth System Sciences*, *18*(10).

Lapena, D. R., & Martz, L. W. (1996). An investigation of the spatial association between snow depth and topography in a Prairie agricultural landscape using digital terrain analysis. *Journal of Hydrology*, *184*(3-4), 277-298.

Lawrence, D. M., & Slater, A. G. (2010). The contribution of snow condition trends to future ground climate. *Climate dynamics*, 34(7-8), 969-981.

Lehning, M., Grünewald, T., & Schirmer, M. (2011). Mountain snow distribution governed by an altitudinal gradient and terrain roughness. *Geophysical Research Letters*, 38(19).

Lemmetyinen, J., Derksen, C., Rott, H., Macelloni, G., King, J., Schneebeli, M., Wiesmann, A., Leppänen, L., Kontu, A. and Pulliainen, J., (2018). Retrieval of effective correlation length and snow water equivalent from radar and passive microwave measurements. *Remote Sensing*, 10(2), 170.

Liston, G. E. (1999). Interrelationships among snow distribution, snowmelt, and snow cover depletion: Implications for atmospheric, hydrologic, and ecologic modeling. *Journal of applied meteorology*, *38*(10), 1474-1487.

López-Moreno, J. I., Revuelto, J., Alonso-González, E., Sanmiguel-Vallelado, A., Fassnacht, S. R., Deems, J., & Morán-Tejeda, E. (2017). Using very long-range terrestrial laser scanner to analyze the temporal consistency of the snowpack distribution in a high mountain environment. *Journal of Mountain Science*, *14*(5), 823-842.

Luce, C. H., Tarboton, D. G., & Cooley, K. R. (1999). Sub-grid parameterization of snow distribution for an energy and mass balance snow cover model. *Hydrological Processes*, 13(12-13), 1921-1933.

Lundquist, J. D., Cayan, D. R., & Dettinger, M. D. (2004). Spring onset in the Sierra Nevada: When is snowmelt independent of elevation?. *Journal of Hydrometeorology*, *5*(2), 327-342.

Lundquist, J. E., Dickerson-Lange, S.E. Lutz, J.A. and Cristea., N.C. (2013). Lower forest density enhances snow retention in regions with warmer winters: a global framework developed from plot-scale observations and modeling, *Water Resources Research*, 49: 6356–6370, https://doi.org/10.1002/wrcr.20504, 2013.

Mazzotti, G., Currier, W. R., Deems, J. S., Pflug, J. M., Lundquist, J. D., & Jonas, T. (2019). Revisiting snow cover variability and canopy structure within forest stands: Insights from airborne lidar data. *Water Resources Research*, *55*(7), 6198-6216.

Maurer, G. E., & Bowling, D. R. (2014). Seasonal snowpack characteristics influence soil temperature and water content at multiple scales in interior western US mountain ecosystems. *Water Resources Research*, 50(6), 5216-5234.

McMichael, C. H., Palace, M. W., & Golightly, M. (2014). Bamboo-dominated forests and pre-Columbian earthwork formations in south-western Amazonia. *Journal of Biogeography*, *41*(9), 1733-1745.

McNay, R.S., Peterson, L.D., and Nyberg., J.B. (1988). The influence of forest stand characteristics on snow interception in the coastal forests of British Columbia. *Canadian Journal of Forest Resources*, 18: 566-573.

Merow, C., Smith, M. J., & Silander Jr, J. A. (2013). A practical guide to MaxEnt for modeling species' distributions: what it does, and why inputs and settings matter. *Ecography*, 36(10), 1058-1069.

Mishra, A. K., & Coulibaly, P. (2009). Developments in hydrometric network design: A review. *Reviews of Geophysics*, *47*(2).

Mohanty, B. P., Klittich, W. M., Horton, R., & Van Genuchten, M. T. (1995). Spatio-temporal variability of soil temperature within three land areas exposed to different tillage systems. *Soil Science Society of America Journal*, *59*(3), 752-759.

Monson, R. K., Lipson, D. L., Burns, S. P., Turnipseed, A. A., Delany, A. C., Williams, M. W., and Schmidt, S. K. (2006). Winter forest soil respiration controlled by climate and microbial community composition, Nature, 439, 711.

Mott, R., Schirmer, M., & Lehning, M. (2011). Scaling properties of wind and snow depth distribution in an Alpine catchment. *Journal of Geophysical Research: Atmospheres*, *116*(D6).

Mott, R., Gromke, C., Grünewald, T., & Lehning, M. (2013). Relative importance of advective heat transport and boundary layer decoupling in the melt dynamics of a patchy snow cover. *Advances in Water Resources*, 55, 88–97. https://doi.org/10.1016/j.advwatres.2012.03.001

Musselman, K., Molotch, N.P., and Brooks., P.D. (2008). Effects of vegetation on snow accumulation and ablation in a mid-latitude sub-alpine forest. *Hydrological Processes*, 22: 2767-2776., doi:10.1002/hyp.7050.

Nakai, Y., Kitahara, H., Sakamoto, T., Saito, T., and Terajima. T., (1993). Evaporation of snow intercepted by forest canopies. Journal of Japan Forest Society, 75: 191-200 (in Japanese with English summary).

New Hampshire State Climate Office (2014). Climate normals (1981-2010) for selected NH cities and towns. www.unh.edu/stateclimatologist/nhnormals.html

Painter, T. H., Berisford, D. F., Boardman, J. W., Bormann, K. J., Deems, J. S., Gehrke, F., ... & Mattmann, C. (2016). The Airborne Snow Observatory: Fusion of scanning lidar, imaging spectrometer, and physically-based modeling for mapping snow water equivalent and snow albedo. *Remote Sensing of Environment*, *184*, 139-152.

Palace, M. W., McMichael, C. N. H., Braswell, B. H., Hagen, S. C., Bush, M. B., Neves, E., ... & Frolking, S. (2017). Ancient Amazonian populations left lasting impacts on forest structure. *Ecosphere*, *8*(12), e02035.

Parikh, R. J., Havens, J. A., & Scott, H. D. (1979). Thermal diffusivity and conductivity of moist porous media. *Soil Science Society of America Journal*, *43*(5), 1050-1052.

Penner, E. (1970). Thermal conductivity of frozen soils. *Canadian Journal of Earth Sciences*, 7(3), 982-987.

Perron, C.J., Bennett, K., & Lee, T.D. (2004). Forest stewardship plan: Thompson farm. NH: University of New Hampshire. Produced by Ossipee Mountain Land Company, West Ossipee, https://colsa.unh.edu/sites/default/files/thompson-farm-plan.pdf.

Peters, J., De Baets, B., Verhoest, N. E., Samson, R., Degroeve, S., De Becker, P., & Huybrechts, W. (2007). Random forests as a tool for ecohydrological distribution modelling. *Ecological Modelling*, 207(2-4), 304-318.

Phillips, S. J., Dudík, M., & Schapire, R. E. (2004). A maximum entropy approach to species distribution modeling. In *Proceedings of the twenty-first international conference on Machine learning* (p. 83).

Phillips, S. J., Anderson, R. P., & Schapire, R. E. (2006). Maximum entropy modeling of species geographic distributions. *Ecological modelling*, 190(3-4), 231-259.

Phillips, S., & Dudík, M. (2008) Modeling of species distributions with Maxent: New extensions and a comprehensive evaluation. *Ecography* (Cop.) 31(2):161–175.

Pflug, J. M., & Lundquist, J. D. (2020). Inferring distributed snow depth by leveraging snow pattern repeatability: Investigation using 47 lidar observations in the Tuolumne watershed, Sierra Nevada, California. *Water Resources Research*, 56(9), e2020WR027243.

Pomeroy, J.W. and Gray. D.M. (1995). Snowcover accumulation, relocation, and management. National Hydrology Research Institute Science Report No. 7. Hydrological Sciences Division, NHRI, Division of Hydrology, University of Saskatchewan. Environment Canada.

Pomeroy, J. W., Gray, D. M., Shook, K. R., Toth, B., Essery, R. L. H., Pietroniro, A., & Hedstrom, N. (1998). An evaluation of snow accumulation and ablation processes for land surface modelling. *Hydrological Processes*, *12*(15), 2339-2367.

Prokop, A. (2008). Assessing the applicability of terrestrial laser scanning for spatial snow depth measurements. *Cold Regions Science and Technology*, *54*(3), 155-163.

Rahmati, O., Pourghasemi, H. R., & Melesse, A. M. (2016). Application of GIS-based data driven random forest and maximum entropy models for groundwater potential mapping: a case study at Mehran Region, Iran. *Catena*, *137*, 360-372.

Redding, T., & Devito, K. (2011). Aspect and soil textural controls on snowmelt runoff on forested Boreal Plain hillslopes. *Hydrology Research*, *42*(4), 250-267.

Reinmann, A. B. and Templer, P. H.: Increased soil respiration in response to experimentally reduced snow cover and increased soil freezing in a temperate deciduous forest, *Biogeochemistry*, 140, 359-371, 2018.

Revuelto, J., López-Moreno, J. I., Azorin-Molina, C., & Vicente-Serrano, S. M. (2014). Topographic control of snowpack distribution in a small catchment in the central Spanish Pyrenees: intra-and inter-annual persistence. *The Cryosphere*, 8(5), 1989-2006.

Roth, T.R. and Nolin. A.W. (2017). Forest impacts on snow accumulation and ablation across and elevation gradient in a temperate montane environment. *Hydrology and Earth System Sciences*, 21: 5427-5442, https://doi.org/10.5194/hess-21-5427-2017.

Saberi, N., Kelly, R., Flemming, M., & Li, Q. (2020). Review of snow water equivalent retrieval methods using spaceborne passive microwave radiometry. *International Journal of Remote Sensing*, *41*(3), 996-1018.

Sanders-DeMott, R., Ouimette, A. P., Lepine, L. C., Fogarty, S. Z., Burakowski, E. A., Contosta, A. R., & Ollinger, S. V. (2020). Divergent carbon cycle response of forest and grass-dominated northern temperate ecosystems to record winter warming. *Global Change Biology*, 26(3), 1519-1531.

Schlögl, S., Lehning, M., & Mott, R. (2018). How are turbulent sensible heat fluxes and snow melt rates affected by a changing snow cover fraction?. *Frontiers in Earth Science*, *6*, 154.

Schmidt, R.A. and D.R. Gluns. (1991) Snowfall interception on branches of three conifer species. *Canadian Journal of Forest Research*, 21:1262-1269.

Schirmer, M., & Lehning, M. (2011). Persistence in intra-annual snow depth distribution: 2. Fractal analysis of snow depth development. *Water Resources Research*, *47*(9).

Schirmer, M., & Pomeroy, J. W. (2020). Processes governing snow ablation in alpine terrain–detailed measurements from the Canadian Rockies. Hydrology and Earth System Sciences, 24(1), 143-157.

Shook, K., Gray, D. M., & Pomeroy, J. W. (1993). Temporal Variation in Snowcover Area During Melt in Prairie and Alpine Environments: Paper presented at the 9th Northern Res. Basin Symposium/Workshop (Whitehorse/Dawson/Inuvik, Canada-August 1992). *Hydrology Research*, *24*(2-3), 183-198.

Singh, V. P. (1997). The use of entropy in hydrology and water resources. *Hydrological processes*, *11*(6), 587-626.

Sorensen, P. O., Finzi, A. C., Giasson, M.-A., Reinmann, A. B., Sanders-DeMott, R., and Templer, P. H. (2018). Winter soil freeze-thaw cycles lead to reductions in soil microbial biomass and activity not compensated for by soil warming, Soil Biology and Biochemistry, 116, 39-47.

Sørensen, R., Zinko, U., and Seibert, J. (2006). On the calculation of the topographic wetness index: evaluation of different methods based on field observations, *Hydrology and Earth System Sciences*, 10, 101–112, https://doi.org/10.5194/hess-10-101-2006.

Starkloff, T., Stolte, J., Hessel, R., and Ritsema, C.: Investigating the development of shallow snowpacks on arable land, using comprehensive field observations and spatially distributed snow modelling, *Hydrology Research*, 49, 41-59, 2017.

Stieglitz, M., Ducharne, A., Koster, R., & Suarez, M. (2001) The impact of detailed snow physics on the simulation of snow cover and subsurface thermodynamics at continental scales. *Journal of Hydrometeorology*, 2(3), 228-242.

Storck, P., Lettenmaier, D.P. and Bolton. S.M. (2002) Measurement of snow interception and canopy effects on snow accumulation and melt in a mountainous maritime climate, Oregon, United States. *Water Resources Research*, 38(11): 1223. https://doi.org/10.1029/2002WR001281

Sturm, M., Goldstein, M. A., & Parr, C. (2017). Water and life from snow: A trillion dollar science question. *Water Resources Research*, *53*(5), 3534-3544.

Sturm, M., & Holmgren, J. (2018). An automatic snow depth probe for field validation campaigns. *Water Resources Research*, 54(11), 9695-9701.

Sturm, M., & Wagner, A. M. (2010). Using repeated patterns in snow distribution modeling: An Arctic example. *Water Resources Research*, 46, W12549.

Tinkham, W. T., Smith, A. M., Marshall, H. P., Link, T. E., Falkowski, M. J., & Winstral, A. H. (2014). Quantifying spatial distribution of snow depth errors from LiDAR using Random Forest. *Remote sensing of environment*, 141, 105-115.

Trujillo, E., Ramírez, J. A., & Elder, K. J. (2007). Topographic, meteorologic, and canopy controls on the scaling characteristics of the spatial distribution of snow depth fields. *Water Resources Research*, *43*(7).

Tucker, C. L., Tamang, S., Pendall, E., and Ogle, K. (2016). Shallow snowpack inhibits soil respiration in sagebrush steppe through multiple biotic and abiotic mechanisms, Ecosphere, 7, e01297.

Yi, Y., Kimball, J. S., Chen, R. H., Moghaddam, M., and Miller, C. E. (2019). Sensitivity of active-layer freezing process to snow cover in Arctic Alaska, The Cryosphere, 13, 197.

Wang, J., & Bras, R. L. (2011). A model of evapotranspiration based on the theory of maximum entropy production. *Water Resources Research*, *47*(3).

Westhoff, M. C., Zehe, E., & Schymanski, S. J. (2014). Importance of temporal variability for hydrological predictions based on the maximum entropy production principle. *Geophysical Research Letters*, *41*(1), 67-73.

Zehe, E., Blume, T., & Blöschl, G. (2010). The principle of 'maximum energy dissipation': a novel thermodynamic perspective on rapid water flow in connected soil structures. *Philosophical Transactions of the Royal Society B: Biological Sciences*, *365*(1545), 1377-1386.

Zhu, D., Ciais, P., Krinner, G., Maignan, F., Puig, A. J., & Hugelius, G. (2019). Controls of soil organic matter on soil thermal dynamics in the northern high latitudes. *Nature communications*, *10*(1), 1-9.